Amphiphilic Water Soluble Triblock Copolymers Based on Poly(2,3-dihydroxypropyl methacrylate) and Poly(propylene oxide): Synthesis by Atom Transfer Radical Polymerization and Micellization in Aqueous Solutions

Elkin Amado,[†] Christian Augsten,[‡] Karsten Mäder,[‡] Alfred Blume,*[,†] and Jörg Kressler*[,†]

Department of Chemistry, Institute of Physical Chemistry, Martin-Luther-University Halle-Wittenberg, D-06099 Halle (Saale), Germany, and Department of Pharmacy, Institute of Pharmaceutics and Biopharmaceutics, Martin-Luther-University Halle-Wittenberg, D-06099 Halle (Saale), Germany

Received April 8, 2006; Revised Manuscript Received October 31, 2006

ABSTRACT: A series of novel water-soluble amphiphilic triblock copolymers having ABA architecture has been synthesized via atom transfer radical polymerization (ATRP) technique. The blocks comprised a thermoresponsive poly(propylene oxide) (PPO) middle block with a molar mass of around 2000 g·mol^{-1} and two hydroxy-functional poly(2,3-dihydroxypropyl methacrylate) (also named poly(glycerol monomethacrylate) (PGMA)) outer blocks with lengths varying from 14 to 221 monomeric units per block, which account for the solubility in water. Gel permeation chromatography analysis confirmed unimodal molar mass distributions with polydispersity indexes ranging between 1.29 and 1.40. Their association behavior in aqueous solutions was studied. The size of the micelles formed and the thermal dependence of the micellization process were followed by dynamic light scattering at different temperatures. Depending on the length of the PGMA blocks, micelles showed an average hydrodynamic diameter in the range from 20 to 30 nm. Critical micellization concentrations (cmc) were determined using surface tension measurements, fluorescent probe technique with pyrene as probe molecule and isothermal titration calorimetry and were found to be in the range from 8×10^{-6} to 2×10^{-4} M depending on the length of the PGMA block and on the method used.

Introduction

Amphiphilic triblock copolymers with sufficiently long blocks and flexible backbones have been found to self-assemble spontaneously into micelles when dissolved in a solvent selective for one of the blocks.[1] If the polymer is water-soluble, such micelles are able to solubilize nonpolar compounds, providing a route for the incorporation of a variety of hydrophobic substances, including drugs, into water-based formulations.[2] Triblock copolymers of the ABA type comprising a poly(propylene oxide) (PPO) middle block and two poly(ethylene oxide) (PEO) hydrophilic outer blocks (also named Pluronic, Poloxamer, or Synperonic) are well-known examples. They are commercially successful as emulsifiers for perfluororganics in blood replacement formulations. They have also been shown to facilitate the permeation of relatively large molecules across lipid bilayers[3] and to act as sensitizing agents for the treatment of multidrug-resistant cancer tumors.[4]

2,3-Dihydroxypropyl methacrylate, also known as glycerol monomethacrylate (GMA), is a highly hydrophilic monomer of commercial interest. Hydrogels based in GMA have already been studied for some years.[5] Due to its increased hydrophilicity, GMA is a candidate for replacing the less hydrophilic 2-hydroxyethyl methacrylate (HEMA) in products such as soft contact lenses, hydrogels, drug delivery, and other medical applications.[6,7] Furthermore, it has been investigated as material for ultrafiltration barriers mimicking the behavior of natural membranes in kidneys.[8]

Anionic polymerization has been traditionally the chosen technique for the preparation of well-defined block copolymers, especially because of the predictable molar masses, exact block compositions and very narrow molar mass distributions, and hence low polydispersities, which can be obtained. However, this technique possesses also the significant drawback of having stringent requirements regarding monomer purity, nearly complete moisture exclusion and demanding polymerization conditions, including very low temperatures. Moreover, the presence of functionalities in the monomers can cause undesirable side reactions and therefore, sometimes the monomer functional groups need to be protected during the polymerization. In fact, HEMA cannot be polymerized by anionic polymerization due to the labile proton on the hydroxy group.[9] In contrast to anionic polymerization, atom transfer radical polymerization (ATRP) technique tolerates well water and other minor impurities and the reaction takes place at a convenient temperature range, typically from 0 to 100 °C, while still yielding polymers with molar masses predetermined by the ratio of monomer to initiator and low polydispersities.[10,11] Also a wide variety of monomers such as styrenes, acrylates and methacrylates have already been successfully polymerized by ATRP.[12]

Poly(glycerol monomethacrylate) (PGMA) homopolymer and copolymers with styrenes, isoprene and some methacrylates have been synthesized before by anionic polymerization of the protected monomer (2,2-dimethyl-1,3-dioxolan-4-yl)methyl methacrylate (DMM), otherwise known as solketal methacrylate (SMA), followed by the hydrolysis of the acetonide protective group.[13−16] On the other hand, GMA monomer has recently been directly homo- and copolymerized by ATRP.[20] However, to the

* Corresponding authors: (J.K.) joerg.kressler@chemie.uni-halle.de; (A.B.) alfred.blume@chemie.uni-halle.de.

[†] Department of Chemistry, Institute of Physical Chemistry, Martin-Luther-University Halle-Wittenberg.

[‡] Department of Pharmacy, Institute of Pharmaceutics and Biopharmaceutics, Martin-Luther-University Halle-Wittenberg.

10.1021/ma060794n CCC: $33.50
Published on Web 12/19/2006

best of our knowledge, there has been only one report of PDMM preparation by ATRP,[21] but not for the synthesis of triblock copolymers.

In this study, a series of novel triblock copolymers with ABA architecture was synthesized by ATRP technique, comprising a PPO middle block and two outer PGMA blocks, which account for the solubility in water. As far as we are aware, there have been no reports dealing with this type of triblock copolymers, in spite of being quite interesting because their behavior in aqueous solutions could be analogous to that of the already mentioned amphiphilic PEO−PPO−PEO triblock copolymers.

In a second stage of this investigation, the micellization behavior of the PGMA−PPO−PGMA triblock copolymers in aqueous solutions was studied. For the application of micelles as nanocarriers, i.e., for incorporating noncovalently hydrophobic substances into the hydrophobic core of the micelle, the problem of their stability upon dissolution is of fundamental importance. The key parameter characterizing the micelle stability during dissolution is the critical micellization concentration (cmc). At a given temperature, micelles are formed at polymer concentrations equal to or exceeding the cmc value. In this study, several independent methods were employed for the determination of the cmc values for the copolymers, namely: surface tension (Wilhelmy plate method), isothermal titration calorimetry (ITC) and a fluorescent probe technique with pyrene as probe molecule. Also the size range of micelles is an important parameter for anticipating the interaction with cells and tissues upon administration in organisms if the micelles were to be used as microcontainers for drug delivery. Therefore, micelle dimensions and the influence of temperature on micellar size were studied by dynamic light scattering.

Experimental Section

Materials. 2,2-Dimethyl-4-hydroxymethyl-1,3-dioxolan (Solketal, 97%), 2,2′-bipyridin (99,5%) and $Cu^{I}Cl$ for analysis were purchased from Merck, methacryloyl chloride (97%), triethylamine (98%) and $Cu^{II}Cl_2$ (97%) were purchased from Fluka. Poly(propylene oxide) dihydroxy-terminated ($M_n \sim 2000$ g·mol^{-1}) and 2-bromoisobutyryl bromide (98%) were purchased from Aldrich.

Monomer Synthesis. (2,2-Dimethyl-1,3-dioxolan-4-yl)methyl methacrylate (DMM) was synthesized from 2,2-Dimethyl-4-hydroxymethyl-1,3-dioxolan and methacryloyl chloride according to a method reported elsewhere.[22] Briefly, freshly distilled triethylamine (59.7 g, 0.61 mol) was mixed in 200 mL benzene with isopropylidene glycerol (80.4 g, 0.61 mol) and cooled to ∼0 °C in a water−ice bath. Methacryloyl chloride (47.7 g, 0.46 mol) was vacuum distilled ($T_b \sim 44$ °C, 70 mbar), diluted in 100 mL benzene and added dropwise along 2 h, with stirring in a water−ice bath under argon atmosphere. The mixture was agitated for 20 h more at room temperature. The reaction mixture was filtered for removing the precipitated triethylamine hydrochloride, and the solution was washed twice with 250 mL distilled water and dried with anhydrous sodium sulfate. After filtration, 0.5 g methylene blue was added and benzene was evaporated under reduced pressure yielding a pale orange liquid. The product was purified by fractional distillation at 66−67 °C (5 mbar) to give 65.8 g (0.33 mol, 72% yield) of (2,2-dimethyl-1,3-dioxolan-4-yl)methyl methacrylate as colorless liquid. Then, 0.5 g methylene blue was added as inhibitor. See Figure 1.

Initiator Synthesis. The ABA triblock copolymer was prepared using an alkyl bromide derivative of poly(propylene oxide) as macroinitiator (PPO−Br) for the polymerization of (2,2-dimethyl-1,3-dioxolan-4-yl)methyl methacrylate by ATRP. The macroinitiator was synthesized by reacting the terminal hydroxy groups of poly(propylene oxide) dihydroxy-terminated ($M_n \sim 2000$ g·mol^{-1}) with excess 2-bromoisobutyryl bromide (BIB) in the presence of triethylamine (TEA) in a molar ratio [PPO]:[BIB]:[TEA] 1:4:4, for 2 days at room temperature, according to literature.[23−25]

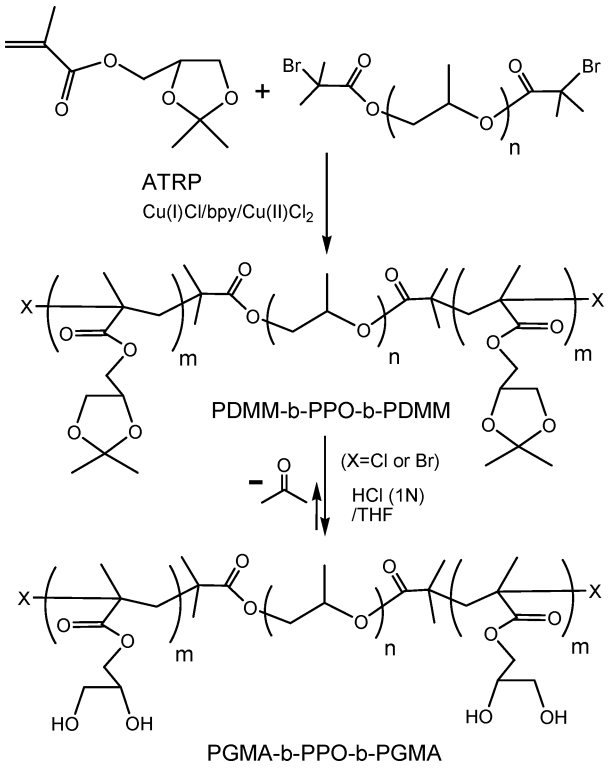

Figure 1. Reaction scheme for the ATRP synthesis of PDMM−PPO−PDMM using a PPO-based macroinitiator and further deprotection reaction for obtaining the PGMA−PPO−PGMA triblock copolymers.

Triblock Copolymer Synthesis. The PDMM−PPO−PDMM triblock copolymers were synthesized following an ATRP method.[26] The PPO−Br macroinitiator was used to polymerize DMM in solution at 40 °C using a $Cu^{I}Cl$ /$Cu^{II}Cl_2$/bpy catalytic system at a molar ratio of [PPO−Br]/[$Cu^{I}Cl$]/[$Cu^{II}Cl_2$]/[bpy] = 1/1/0.2/2.5. In a typical procedure $Cu^{I}Cl$ and $Cu^{II}Cl_2$ were pestled and added together with bpy into a Schlenk flask equipped with a stirring bar. This flask was then sealed with a rubber septum, evacuated, and filled with dry argon (three cycles). DMM was freshly vacuum distilled for removing the inhibitor and syringed into the reaction flask. The mixture was degassed via three freeze−thaw cycles. A solution of the PPO−Br macroinitiator dissolved in isobutyl acetate, which was freshly distilled from CaH_2, was separately degassed and transferred into the reaction flask under argon via a double-tipped needle. The added solvent was enough for getting a 20% v/v DMM solution in isobutyl acetate. After stirring, a dark brown reaction mixture was obtained. The temperature was increased to 40 °C and the polymerization commenced. To monitor the extent of polymerization of DMM, 1 mL aliquots were taken at regular intervals, quenched and immediately filtered through silica gel columns to remove the catalyst. A small amount of the filtrate was diluted with THF and evaluated by GPC. The reaction mixture was stirred for 20 h and then exposed to air while cooling. Termination occurred rapidly as indicated by the color change from brown to green due to the aerial oxidation of Cu(I) to Cu(II). The reaction mixture was then passed through a silica gel column to remove the copper catalyst. After the solvent was evaporated off, the polymer was dissolved in THF and precipitated three times into cold hexane. After drying in a vacuum oven at room temperature a white, slightly yellow powder was obtained.

Deprotection of PDMM—PPO—PDMM Triblock Copolymer. In a typical procedure,[14,15] the solution of PDMM−PPO−PDMM triblock copolymer (2.5 g) in THF (25 mL) was cooled in a water−ice bath and aqueous 1 N HCl (10 mL) was added dropwise. The solution became turbid on addition of aqueous HCl

and was stirred at room temperature for 24 h. As the reaction proceeds the solution becomes gradually clear. The solution was poured into hexane−ethanol (10:l) to precipitate the polymer, which was again reprecipitated from THF−methanol (1:4) to hexane−ethanol (4:l). Finally the deprotected polymer PGMA−PPO−PGMA was dried in a vacuum oven yielding a white powder.

Characterization. Gel Permeation Chromatography (GPC). Molar masses and molar mass distributions were assessed by GPC using THF as the mobile phase for the protected copolymers and water (GC Grade) for the deprotected ones. The GPC setup comprised a Knauer apparatus coupled with a refractive index detector. Two Macherey-Nagel columns were used. The flow rate for the eluent was set at 1.0 mL·min^{-1}. The columns working with THF were calibrated with a series of narrowly distributed poly(methyl methacrylate) standards, covering the M_w range from 500 to 400000 g·mol^{-1}. The columns working with water were calibrated with PEO standards, covering the M_w range from 1500 to 23000 g·mol^{-1}.

NMR and IR Spectroscopy. ^{1}H NMR and ^{13}C NMR spectra were recorded on a Varian Inova 500 spectrometer in DMSO-d_6 (500 MHz for ^{1}H spectra, 100 MHz for ^{13}C spectra). Infrared (FTIR) analysis was performed on pressed KBr and spectra were recorded using a Bruker Vector 22 spectrometer.

Dynamic light scattering (DLS) measurements in the high-temperature range, 15−45 °C, were performed using a commercial equipment, ALV−NIBS/HPPS from ALV−Laser (Langen, Germany), which features a back scattering detection at a fixed scattering angle of 173°. The light source is a He−Ne laser (λ_0 = 632.8 nm) with a power output of 3 mW. For measurements in the low-temperature range, 4−20 °C, the equipment used was an ALV goniometer equipped with a Nd/YAG DPSS-200 laser (λ_0 = 532.8 nm) which enables measurements between 20 and 150°. The sample solutions were prepared in deionized water and filtered through 0.20 μm pore size filters into 1.5 mL volume cuvettes. The signal analyzer was an ALV-5000/E digital multiple-τ correlator. The correlation functions were analyzed by the CONTIN method, giving information on the distributions of decay rate (Γ). Apparent diffusion coefficients were obtained from $D_{app} = \Gamma/q^2$ [with $q = (4\pi n_o/\lambda)\sin(\theta/2)$ being the scattering vector, n_o = refractive index of the medium, λ = wavelength of the light, θ = scattering angle] and the corresponding apparent hydrodynamic radii, R_h (radius of the hydrodynamically equivalent sphere), were obtained via the Stokes−Einstein equation $R_h = kT/(6\pi\eta D_{app})$, where k is the Boltzmann constant and η is the viscosity of the solvent, water in this case, corrected at the temperature T.

Multiangle light scattering (MALS) in water was employed for obtaining absolute molar masses and micellar aggregation numbers (N_{agg}) after separation of the sample in fractions by asymmetrical flow field−flow fractionation (AF4). The details about these measurements are given in the Supporting Information.

Isothermal Titration Calorimetry (ITC). Heat of demicellization and dilution were measured using a VP−ITC titration microcalorimeter (MicroCal, Northampton, MA). The sample cell had a volume of 1.45 mL. It was filled with degassed water prior to each experiment. Polymer solutions with a concentration of around 30 times cmc were placed in a 250 μL continuously stirred (310 rpm) syringe. 50 aliquots (5 μL each) were injected into the sample cell at intervals of 480 s. Data analysis was carried out using Microcal ORIGIN software.

Fluorescence Measurements. Steady-state fluorescent spectra were measured using a Fluoromax 2 spectrometer (Jobin-Yvon) with a slit width of 0.5 mm (Band-pass 2.125 nm) for both excitation and emission spectra. For the measurements, 1.5 mL of solution was placed in a 1.0 × 1.0 cm cell. All spectra were run on air-equilibrated solutions. For fluorescence emission spectra, λ_{ex} was 333 nm, and for excitation spectra, λ_{em} was 390 nm. Spectra were accumulated with an integration time of 0.1 s. Samples with a pyrene concentration of 5.4 × 10^{-7} M were prepared according to literature methods,[27] and they were incubated at the measuring temperature for at least 24 h.

Surface Tension Measurements. The surface tension (γ) was measured by the Wilhelmy plate method, using a DCAT11 tensiometer (DataPhysics Instruments GmbH, Filderstadt, Germany) at 40 °C. The temperature (±0.1 °C) was maintained by circulating thermostated water through the jacketed vessel containing the solution. The concentration of solution was varied by adding aliquots of stock solution of concentration of around 30 × cmc through an automatic injection system. The plate was previously cleaned by heating it in a flame.

Adsorption Kinetics at the Air—Water Interface. Adsorption experiments were performed using a round home-built Teflon trough with a total area of 7.07 cm^2 and a volume of 11.3 mL. Polymer solutions were injected below the subphase with a Hamilton syringe through a Teflon jacket just above the bottom of the trough. The subphase was stirred with a tiny rolling sphere to ensure a homogeneous distribution of the sample without perturbing the surface. The increase of surface pressure due to the injected triblock copolymer was measured by the Wilhelmy plate method. The temperature of the subphase was maintained at 40 °C by circulating thermostated water through the jacketed vessel containing the solution and inside the walls of a covering hood designed to minimize water evaporation.

Results and Discussion

Triblock Copolymer Synthesis. Although GMA monomer has already been directly copolymerized by ATRP,[17−20] the high polarity of GMA and of the obtained PGMA makes it necessary to use very polar solvents, such as DMF, DMSO or methanol, to dissolve them, which can dramatically affect the structure and function of the catalytic species involved in ATRP.[9] Besides, due to the synthetic routes used to produce GMA, the commercial "monomer" contains in reality as much as 8% of 1,3-dihydroxypropyl methacrylate impurity, which leads after the polymerization to statistical copolymers rather than homogeneous PGMA homopolymers or blocks.[28] Consequently, in this study the protected monomer DMM was used instead, which allows to apply for the ATRP procedure similar conditions to the ones used for the thoroughly studied and well documented ATRP of methyl methacrylate (MMA).[29−31]

The choice of a 2-bromoisobutyrate for the alkyl bromide initiator was based on the finding that, since it is close in imitating the structure of the propagating methacrylate chain end it has been employed successfully in the ATRP synthesis of polar methacrylate monomers as shown by Beers et al.[9] It has also been shown that the use of a mixed halide initiator/catalyst system of the type R−Br/Cu^{I}Cl, that is, alkyl bromide initiators in combination with copper chloride catalyst, exhibits faster initiation than the R−Cl/CuCl system and slower propagation than R−Br/CuBr. A fast rate of initiation relative to the rate of propagation is essential for a successful controlled radical polymerization. Moreover, due to the carbon−chlorine bond being stronger than the corresponding carbon−bromine bond there is a tendency of the polymer chain ends to be terminated by chlorine instead of bromine.[31] Additionally, side reactions observed in R−Br/Cu^{I}Br-initiated ATRP of MMA causing the deviation of molar mass as a function of conversion[32] could be minimized with the mixed halide initiator/catalyst system, leading to better control over the molar mass at high conversions of monomer to polymer.

A ligand/Cu^{I}Cl molar ratio of 2 has been used because although the rate of ATRP polymerization of MMA using copper(I) halide/R−X systems reaches a maximum when the ligand/Cu^{I}Cl molar ratio equals approximately 1, the reaction mixture requires too long to become homogeneous for an equimolar ratio, while copper(I) halides dissolve much faster when an excess of ligand is used.[30] Finally, Cu^{II}Cl$_2$ was

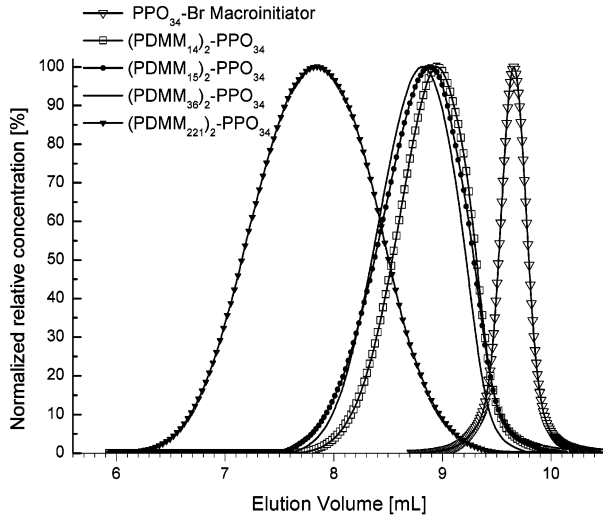

Figure 2. GPC chromatograms in THF for the PPO_{34}−Br macroinitiator and the synthesized PDMM−PPO−PDMM triblock copolymers.

Table 1. Polydispersities, Molar Masses, and Degree of Polymerization for the PGMA−PPO−PGMA Triblock Copolymers and Micellar Apparent Hydrodynamic Radii (R_h) in the Temperature Range 15−40 °C from DLS

sample	M_w/M_n[a]	m[b] (^{1}H NMR)	M_n (^{1}H NMR) [g/mol]	R_h [nm]
$(PGMA_{221})_2-PPO_{34}$	1.39	221	73 000	∼50
$(PGMA_{36})_2-PPO_{34}$	1.29	36	13 600	11.4 ± 1.8
$(PGMA_{15})_2-PPO_{34}$	1.40	15	6600	14.0 ± 3.0
$(PGMA_{14})_2-PPO_{34}$	1.32	14	6400	10.2 ± 1.4

[a] GPC of PDMM−PPO−PDMM in THF, PMMA standards. [b] Degree of Polymerization per PGMA block from ^{1}H NMR in DMSO-d_6.

added in a low molar ratio ($[Cu^{II}Cl_2]_0/[Cu^{I}Cl]_0 = 0.2$) to the reaction mixtures to increase the initial concentration of the deactivating species in solution, so as to reduce the concentration of propagating radicals and the amount of irreversible termination. The reaction scheme for the ATRP synthesis of the PGMA−PPO−PGMA triblock copolymer is outlined in Figure 1.

The GPC chromatograms in THF for the initial PPO_{34}−Br macroinitiator and the obtained PDMM−PPO−PDMM triblock copolymers are shown in Figure 2. All copolymers showed a symmetrical, monomodal molar mass distribution. The absence of more than one peak or tailing on the elution curve shows that neither homopolymers, nor diblock copolymers were produced during the polymerization. Thus, it can be claimed that only triblock copolymers were obtained. The polydispersities were quite acceptable ranging from 1.29 to around 1.40; see Table 1. Figure 3 shows typical ^{1}H NMR spectra obtained for the PGMA−PPO−PGMA triblock copolymer before (a) and after (b) the deprotection reaction. The degree of polymerization for the PGMA blocks, m, is calculated from the ratio between the integral of the peak corresponding to the methyl group from the PPO block (peak 1, integral I_1 ,3H) and the integral of the peak corresponding to the methyl groups from both PGMA blocks (peak f, integral I_f ,6H) according to the equation: $m = (I_f \times n)/(2 \times I_1)$, being the degree of polymerization for the PPO, $n = 34$. On the other hand, it was found that, when the spectra are recorded in DMSO-d_6, clear peaks for each hydroxy group (−OH) of the PGMA block are obtained at 4.64 ppm (CH_2 O***H***, peak a, integral I_a ,1H) and at 4.88 ppm (CH_2 CH-(O***H***)CH_2, peak a′, integral $I_{a'}$, ,1H). These signals are well

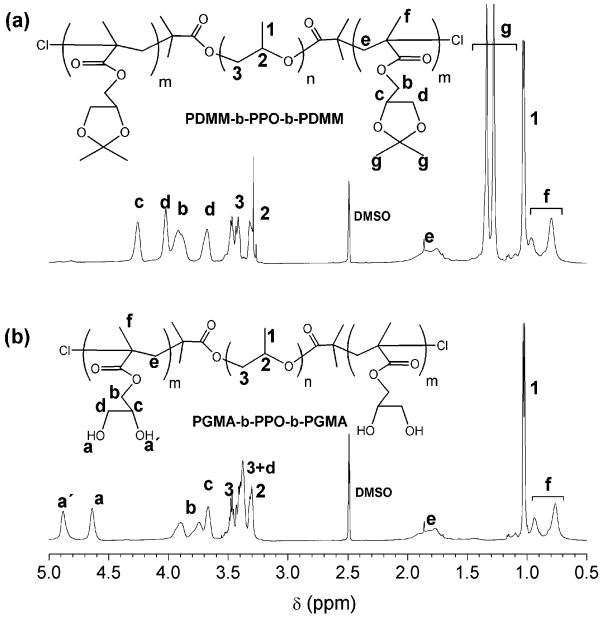

Figure 3. ^{1}H NMR spectra (500 MHz in DMSO-d_6): (a) $(PDMM_{14})_2-PPO_{34}$ protected triblock copolymer; (b) $(PGMA_{14})_2-PPO_{34}$ after the deprotection reaction (HCl 1 N, 24 h at room temperature).

separated from the backbone peaks and do not shift or broaden as could be expected in other solvents. From the integrals for these peaks, similar values for m are obtained according to the equation : $m = [(I_a + I_{a'}) \times 1.5 \times n]/(2 \times I_1)$. Having m, the average molar masses of the original PDMM−PPO−PDMM triblock copolymers were calculated and compared with values obtained from GPC (see Supporting Information). The differences between the M_n values obtained from both methods were quite considerable (GPC values were as high as twice the ^{1}H NMR values for the two shortest copolymers). This is partially due to the fact that PMMA homopolymers were used as standards for GPC calibration. Because of the bulky acetonide ring the hydrodynamic volumes of both polymers at the same molar masses are presumably too different. Large disagreements between GPC and ^{1}H NMR measurements in similar situations have been reported before.[9,16] Moreover, it is also possible that inside the GPC column additional effects, such as partitioning, were present besides the desired size exclusion separation mechanism.[33] Furthermore, it is uncertain that THF is a completely nonselective solvent for both of the blocks (PDMM and PPO). Thus, the elution behavior of the block copolymers may strongly depend on composition.

Removal of the Acetal Protecting Group. The 1,3-dioxolane ring in PDMM−PPO−PDMM was readily cleaved to regenerate the diol function by treating the copolymer with 1 N HCl in THF at room temperature for 24 h. In the ^{1}H NMR spectra of PGMA−PPO−PGMA (Figure 3), the methyl proton signals of the 1,3-dioxolane ring at 1.28 and 1.34 ppm ($C(C\boldsymbol{H}_3)_2$) thoroughly disappeared after deprotection of PDMM−PPO−PDMM. Likewise, in the ^{13}C NMR spectra (Figure 4) the carbon signals of the dioxolane ring at 108.78 ppm (O***C***O) and at 25.15 and 26.46 ppm ($C(\boldsymbol{C}H_3)_2$) also disappeared.

Figure 5 shows the comparison between FTIR spectra in KBr of the PGMA−PPO−PGMA triblock copolymer before (a) and after (b) the deprotection reaction. A very strong OH stretching band due to the diol function appeared after deproctection at 3000−3750 cm^{-1}. Also a new band at 1119 cm^{-1} corresponding to the (**C**−**O**) stretching vibration from a secondary alcohol is observed. The deformation bands due to the geminal methyl

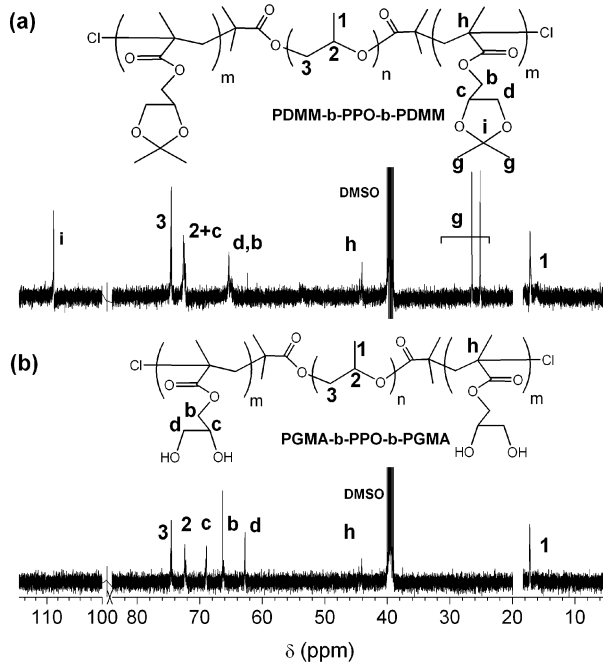

Figure 4. ^{13}C NMR spectra (100 MHz in DMSO-d_6): (a) $(PDMM_{15})_2-PPO_{34}$ triblock copolymer; (b) $(PGMA_{15})_2-PPO_{34}$ after the deprotection reaction (HCl 1 N, 24 h at room temperature).

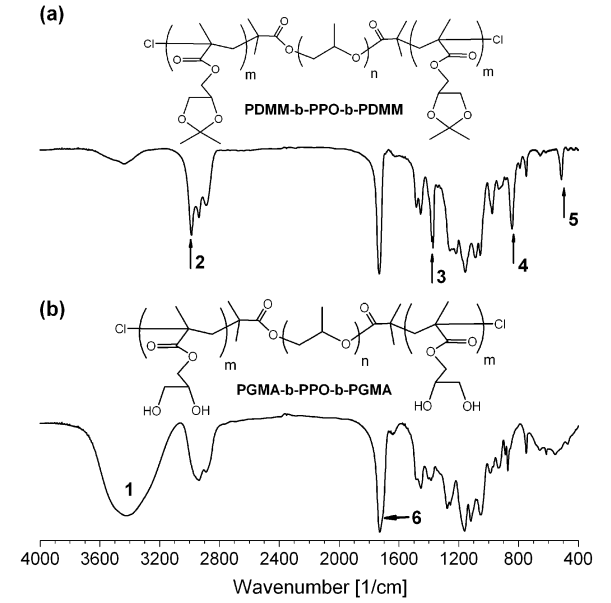

Figure 5. FTIR spectra in KBr (a) $(PDMM_{36})_2-PPO_{34}$ triblock copolymer (b) $(PGMA_{36})_2-PPO_{34}$ after the deprotection reaction (HCl 1 N, 24 h at room temperature). The peaks marked are derived from the following: diol group (**1**, 3000−3750 cm^{-1}); geminal methyl groups on acetonide ring (**2**, 2988 cm^{-1}, and **3**, 1372, 1382 cm^{-1}); acetonide ring (**4**, 842 cm^{-1}, and **5**, 513 cm^{-1}); carbonyl group (**6**, 1728 cm^{-1}).

group of the dioxolane ring ($C(\mathbf{CH_3})_2$) at 1372−1382 cm^{-1} (doublet) almost disappeared after deprotection. Accordingly, the methyl ($-\mathbf{CH_3}$) asymmetrical stretching band at 2988 cm^{-1} decreased significantly. The characteristic carbonyl (**C═O**) stretching band shifted from 1733 cm^{-1} to lower frequencies 1728 cm^{-1}. This shift has been ascribed before to hydrogen bonding between the carbonyl and diol groups in the deprotected polymers.[34,14] Also the disappearance of the peaks at 513 and 842 cm^{-1} coming from the acetonide ring is in agreement with the removal of the protecting group. On the other hand, while the (**C−O−C**) stretching absorption at 1087 cm^{-1} coming from

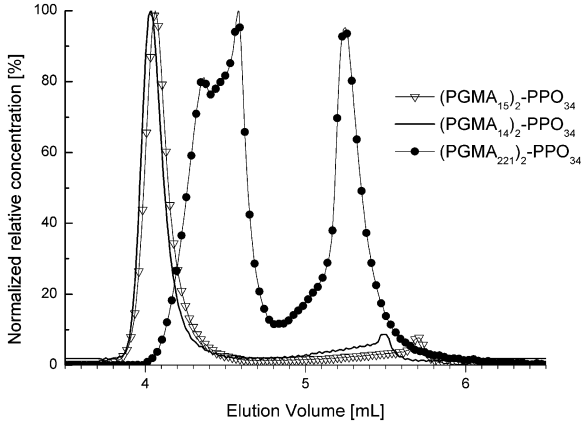

Figure 6. GPC chromatograms in water for the deprotected PGMA−PPO−PGMA triblock copolymer. Concentration 1% w/w.

only the acetal group disappears, the (**C−O−C**) stretching absorption coming from both the ester and acetal groups at 1055 cm^{-1} is still present after the deprotection reaction. Therefore, it is concluded that the ester group remained intact during the hydrolysis of the acetonide ring.

In conclusion, both NMR and FTIR results verify that the complete removal of the acetonide protecting group was achieved. All PGMA−PPO−PGMA copolymers obtained were soluble in water, methanol and DMSO and insoluble in hexane, THF, chloroform and ethanol. In contrast, PDMM−PPO−PDMM copolymers were insoluble in water and soluble in THF and chloroform, which indicates that the presence of the two hydroxy groups on the repeating unit of PGMA−PPO−PGMA enhanced the hydrophilicity significantly.

Association of PGMA—PPO—PGMA in Water. GPC Measurements. GPC has already been used to detect aggregates and study micellization, due to its ability for detecting hydrodynamic size distributions, based on the differences in hydrodynamic radii. In particular, GPC has been applied for the determina-tion of the relative amounts of micelles and unimers (single chains) as well as the size distribution of micelles.[35] However, it must be kept in mind that GPC suffers from the complex problem of solution dilution inside the columns, which can disturb micellization equilibriums during the measurement and originate misleading results.

The GPC chromatograms in water for the deprotected PGMA−PPO−PGMA triblock copolymers (1% w/w aqueous solutions) are shown in Figure 6. The chromatograms of all samples show two separated peaks, which unfortunately lay outside the calibration range of the columns. The peak at shorter elution times (higher molar masses) might correspond to associated species, micelles or aggregates. The second peak corresponds probably to triblock copolymers unimers. However, a further analysis coming from more suitable techniques such as DLS was necessary to interpret quantitatively these results. Nevertheless, micellization or association in water was already evidenced by these GPC measurements.

DLS Studies. GMA homopolymer is highly hydrophilic and exhibits no lower critical solution temperature (LCST) in aqueous solution.[19,28] It is also water-soluble over the whole pH range at room temperature.[18] On the other hand, the PPO block exhibits LCST phase behavior with the cloud point temperature being dependent on its molar mass. In the case of PPO_{34}, the cloud point is at around 10 °C. At this temperature the PPO block becomes less soluble in water, and is expected to trigger a self-assembly process which should lead to the

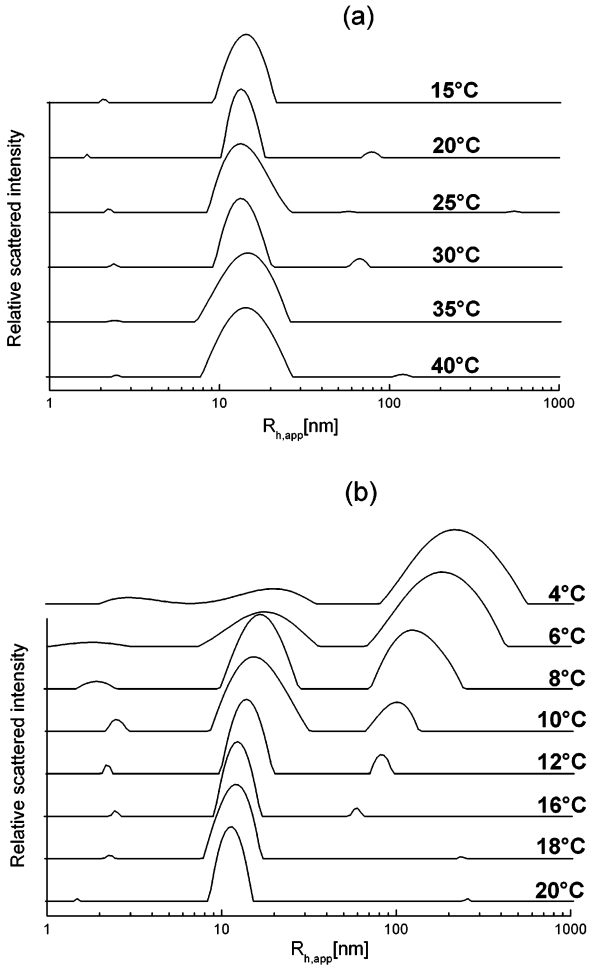

Figure 7. Distributions of apparent hydrodynamic radii (R_h) for (a) $(PGMA_{15})_2-PPO_{34}$ triblock copolymer, 7.0 mM, temperature range 15−40 °C, and (b) $(PGMA_{14})_2-PPO_{34}$, 1.4 mM, between 4 and 20 °C.

formation of micelles with PPO cores and PGMA coronas. In spite of this, the PPO block is still sligthly soluble even at 20 °C, so well-defined micelles are not expected to form at ambient temperature. Moreover, also other aggregation morphologies are possible. It has already been shown, for triblock copolymers with ABC architecture, that an outer PGMA block is effective in minimizing intermicellar fusion at high polymer concentrations, however some micellar aggregation phenomena at elevated temperatures (>40 °C) have been reported and are believed to involve intermicelle hydrogen bonding.[17] From these considerations the PGMA−PPO−PGMA triblock copolymers were expected to be thermoresponsive in aqueous solution since the GMA block is permanently hydrophilic, whereas the PPO block becomes increasingly insoluble at higher temperatures. The specific behavior would depend on the ratio of molar masses between both types of blocks.

From the DLS measurements, the distributions of apparent hydrodynamic radii (R_h) were obtained by nonlinear fitting of the intensity correlation functions. In order to confirm that the signals detected are really originated in translational diffusion processes, an angular dependent measurement of the decay rates (Γ) between 30 and 140° was performed at 30 °C. The linear relationships obtained between Γ and the square of the scattering vector, q^2 (see Supporting Information for details), confirm that the observed peaks are due to diffusive processes.

Figure 7 shows the scattered intensity per particle size class for the $(PGMA_{14})_2-PPO_{34}$ and $(PGMA_{15})_2-PPO_{34}$ triblock copolymers at concentrations of around 12 × cmc and 40 ×

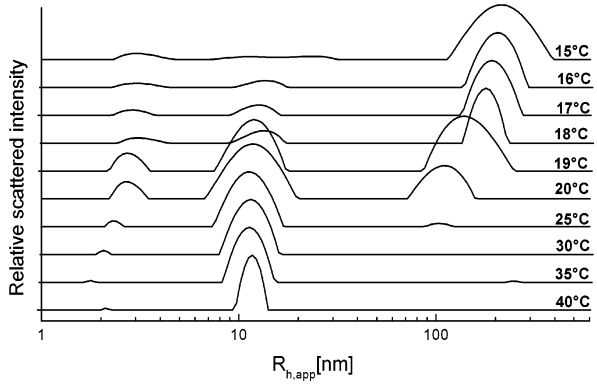

Figure 8. Distributions of apparent hydrodynamic radii (R_h) in the temperature range 15−40 °C for $(PGMA_{36})_2-PPO_{34}$ triblock copolymer at 1 mM concentration.

cmc, respectively (see below for cmc determination). In the high-temperature range (Figure 7a) the distributions for micelles exhibit well-defined and relatively narrow peaks. This contrasts to a recent report by Rannard et al.,[17] who found a huge size decrease with increasing temperature (from R_h = 35 to 15 nm for 30 and 70 °C respectively) for micelles formed by a $PGMA_{50}-PDMA_{20}-PPO_{36}$ triblock copolymer. They explained such contraction as due to progressive dehydration of the PPO core. In our case the size of the micelles remains approximately constant in the high-temperature range, $R_h = 10.2 \pm 1.4$ nm for $(PGMA_{14})_2-PPO_{34}$ and $R_h = 14.0 \pm 3.0$ nm for $(PGMA_{15})_2-PPO_{34}$, and no evidence of remarkable micelle contraction was found. Nevertheless the weight fraction of the copolymer present as micelles (see the corresponding mass weighted distributions of R_h in the Supporting Information) does change significantly with increasing temperature growing from 30.0% w/w at 15 °C up to 91.4% w/w at 40 °C for $(PGMA_{14})_2-PPO_{34}$ and from 19.6% w/w at 15 °C up to 75.5% w/w at 40 °C for $(PGMA_{15})_2-PPO_{34}$. This temperature-dependent micellization is attributed to the increasing insolubility of the PPO block with increasing temperatures, which favors micelle formation. Besides, unimers sizes were approximately the same for both copolymers: $R_h = 2.1 \pm 0.5$ nm for $(PGMA_{14})_2-PPO_{34}$ and $R_h = 2.1 \pm 0.4$ nm for $(PGMA_{15})_2-PPO_{34}$. In the low-temperature range (Figure 7b), when the temperature is lowered down to 4 °C the micelle peak disappears almost completely (when the mass weighted distribution is considered). It amounts to less than 1% w/w of the total copolymer, which indicates that most of the triblock copolymer was molecularly dissolved in water at this temperature. The mass fraction of micelles in comparison to unimers was significant only above 8 °C (3.4% w/w) and increased steadily up to 32.4% w/w at 20 °C. Therefore, 8 °C corresponds approximately to the critical micellization temperature (cmt) for $(PGMA_{14})_2-PPO_{34}$ at a concentration of 1.4 mM.

In the case of $(PGMA_{36})_2-PPO_{34}$ (Figure 8), although an approximately constant value of $R_h = 11.4 \pm 1.8$ nm for the micelles is observed between 20 and 40 °C, at lower temperatures the micelles peak decreases drastically and amounts to only 1.7% w/w of the total copolymer at 15 °C. The cmt for $(PGMA_{36})_2-PPO_{34}$ at a concentration of 1 mM was found to be around 19 °C. For the unimers peak $R_h = 2.5 \pm 0.4$ nm, which is slightly higher than the value obtained for the shorter triblocks.

On the other hand, one additional population with $R_h \sim 175-215$ nm is observed between 15 and 20 °C, which is not be attributed to micelles but to some kind of aggregates. This population corresponds to a fraction of 1.0−1.5% w/w of the

Table 2. Comparison of Cmc Values as Determined from Surface Tension, Isothermal Titration Calorimetry, and Fluorescence Measurements along with Thermodynamic Parameters for the Micellization of PGMA−PPO−PGMA Triblock Copolymers Derived from ITC Data at 40 °C

	cmc		ITC			
sample	Wilhelmy−Platte [M]	fluoresc [M][a]	cmc [M]	$\Delta H°$ micell. [kJ/mol]	$\Delta G°$ micell. [kJ/mol]	$\Delta S°$ micell. [kJ/mol·K]
$(PGMA_{221})_2-PPO_{34}$		2.1×10^{-5}				
$(PGMA_{36})_2-PPO_{34}$	1.1×10^{-5}	8.1×10^{-6}	1.9×10^{-5}	44.99	−38.78	0.27
$(PGMA_{15})_2-PPO_{34}$	1.7×10^{-4}	$<6.7 \times 10^{-6}$	1.1×10^{-4}	7.25	−34.18	0.13
$(PGMA_{14})_2-PPO_{34}$	1.1×10^{-4}	$<2.1 \times 10^{-6}$	5.2×10^{-5}	11.57	−36.13	0.15

[a] Determined from the intensity ratio I_{336}/I_{334} in pyrene excitation spectra.

total and disappears completely above 20 °C, simultaneously with a significant increase in the micelle population. This observation suggests that above the cmt micelles are formed, at least partially, at expense of the dissociation of the aggregates. Armes and co-workers proposed that in the case of PPO−PGMA diblock copolymers the presence of similar aggregates might be due to clustering of micelles.[28] On the contrary, we believe that the aggregation process might be due to intra- and intermolecular hydrogen bonding of adjoining hydroxy groups, in a way similar to what is observed for other highly hydroxylated polymers such as poly(vinyl alcohol) (PVA).[36] For PVA the strong hydrogen bonding originates a remarkable decrease in its solubility in water.[37] Consequently, DLS experiments were performed on aqueous solutions of PGMA homopolymer ($PGMA_{75}$ and $PGMA_{104,}$ 1 mM). Aggregates with R_h ranging from 60 to 100 nm depending on temperature were found. However such aggregates corresponded to around 0.05% w/w of the total homopolymer present and therefore only a tendency to aggregation could be evidenced for the homopolymers.

For $(PGMA_{221})_2-PPO_{34,}$ bearing a considerably larger PGMA block, a multimodal distribution with two or even three populations was observed depending on temperature. In the whole temperature range (15−45 °C) mostly unimers ($R_h \sim$ 4.5 nm) were present. However, also aggregates ($R_h \sim 240$ nm) below 30 °C and micelles ($R_h \sim 50$ nm) above 25 °C, corresponding to a maximum of 0.5% w/w of the total population, were found. This temperature-dependent process is similar to the one described for $(PGMA_{36})_2-PPO_{34}$, but micelles and aggregates fractions are minor compared to unimers for the largest PGMA block, while the cmt is about 25 °C for $(PGMA_{221})_2-PPO_{34}$ at a concentration of 1.1 mM.

The weight-average contour length (L_w) of the PGMA blocks can be estimated by multiplying the degree of polymerization per block derived from ^{1}H NMR measurements by the polydispersities found from GPC (Table 1) and the extended length of a monomeric vinyl unit (2.546 Å).[38] One obtains 4.65, 5.16, 11.9, and 78.3 nm, for 14, 15, 36, and 221 PGMA units respectively. The radius of the PPO core can be estimated, under the assumption that the micelles are spherical in shape and their core is formed by condensed (liquidlike) PPO blocks, from the equation[39]

$$R_{core} = \sqrt[3]{\frac{3nN_{agg}M_{PO}}{4\pi N_A \rho_{po}}} \quad (1)$$

where n is the degree of polymerization of the PPO block ($n =$ 34), M_{PO} is the molar mass of the oxypropylene unit ($M_{PO} =$ 58 g/mol), ρ_{PO} is the density of liquid PPO ($\rho_{PO} = 1.01$ g/cm^3), N_{agg} is the micellar aggregation numbers (N_{agg}=31, 40, and 32 respectively, see Supporting Information) and N_A is the Avogadro's constant. A value of about 3 nm is obtained for all samples. This estimate neglects the possible penetration of water and PGMA into the micelle core and gives therefore a lower limit for the core size. Adding this value to the L_w of the PGMA blocks one obtains 7.7, 8.2, 14.9, and 81.3 nm as radii for the micelles having 14, 15, 36, and 221 PGMA units per block respectively. Comparing these values with the R_h values from DLS (10.2, 14.0, 11.4, and 50 nm, respectively), they are in agreement with the PGMA blocks being coiled to some extent in the corona of the micelle for the longest and intermediate PGMA blocks and would imply a highly improbable all-trans conformation for the two shortest blocks. Therefore, it must be concluded that the PPO core of the micelles is not found in the assumed condensed liquidlike state, but in a hydrated and expanded state, which can also be expected due the partial, although slight solubility of the PPO block in water. Similar conclusions have been drawn from studies of Poloxamer 184, a PEO−PPO−PEO ABA triblock copolymer having a PPO middle block of ~30 propylene oxide units.[40] The length of the propylene oxide unit in a fully extended configuration, assuming bond angles of 110° together with the characteristic bond length for carbon−carbon bonds (1.54 Å) and for carbon-oxygen bonds (1.43 Å), is calculated as 3.60 Å and the contour length of a PPO chain with $n/2$ units ($n = 34$) equals 6.12 nm which is an upper limit for the core size. Adding this value to the L_w of the PGMA blocks, the radii for the micelles obtained are 10.8, 11.3, 18.0, and 84.4 nm. Although these values are in better agreement with the experimental DLS R_h values, they are still a little too low especially for the two relatively short triblocks. There are some possible explanations for this discrepancy between L_w and experimental R_h values: in the first place, the occurrence of a transition from spherical micelles to cylindrical micelles for the shorter members of this homologous series is possible. Such a transition has been described and discussed before for dilute solutions of ABA triblock copolymers of the type PEO−PPO−PEO, for example $EO_{27}-PO_{39}-EO_{27}$.[41] The transition occurs when, as a consequence of an increase in $N_{agg,}$ the radius of the micelle core exceeds the stretched length of half the hydrophobic core and is favored if the hydrophilic blocks are short (which leads to high association numbers) and if the hydrophobic blocks are also short (which sets a low limit on the radius of a spherical micelle).[42] In this study the highest discrepancy between L_w and R_h is shown precisely by the $(PGMA_{15})_2-PPO_{34}$ triblock which is also the one having the biggest association number (N_{agg}=40, vs 31 and 32 for $(PGMA_{14})_2-PPO_{34}$ and $(PGMA_{36})_2-PPO_{34}$ respectively). The second factor playing a role is the polydispersity. By studying the factors influencing the anomalous micellization behavior of Poloxamer 184, it has been unambiguously concluded by Zhou et al.[42] that the origin of such perturbations is the polydispersity of the copolymers. The combination of these two effects could explain the considerable difference in R_h between the $(PGMA_{15})_2-PPO_{34}$ and $(PGMA_{14})_2-PPO_{34}$ triblocks: the former has also the highest polydispersity of all samples, 1.40 vs 1.32 for the latter.

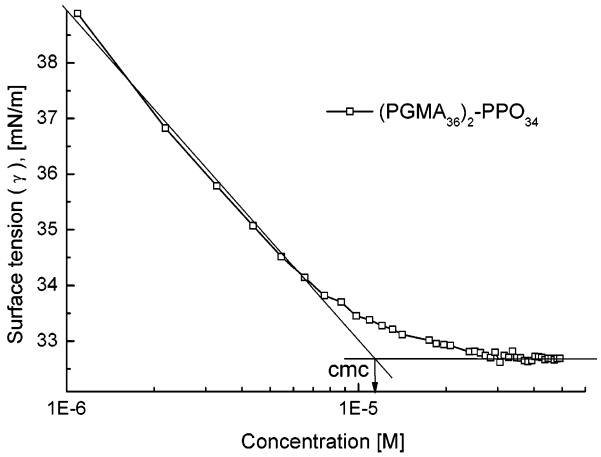

Figure 9. Determination of cmc from the experimental surface tension (γ) vs logarithm of surfactant concentration (log C) for $(PGMA_{36})_2-PPO_{34}$ in water at 40 °C.

Cmc Determination. Surface Tension Measurements. This method relies on the fact that an increase in surfactant concentration leads to a decrease in the surface tension; the micelle formation at the cmc causes a break in this dependence. The measured surface tension values were plotted as a function of logarithm of surfactant concentration and the cmc value was determined by the crossing point of the straight lines that continue the surface tension vs log concentration curves before and after the break. A representative plot of surface tension (γ) vs logarithm of surfactant concentration (log *C*) for $(PGMA_{36})_2-PPO_{34}$ is shown in Figure 9. The cmc values determined according to this method are given in Table 2

Adsorption Kinetics at the Air—Water Interface. To obtain information about the adsorption behavior of the triblock copolymers at the air/water interface, different volumes of an aqueous solution of the copolymer were injected into the water-filled trough, and the subsequent increase in surface pressure was monitored.[43] The surface tension γ is directly measured using the Wilhelmy plate method and relates to the surface pressure π by $\pi = \gamma_0 - \gamma$ where γ is the surface tension for a monolayer-covered water surface and γ_0 is the surface tension of the neat water surface ($\gamma_0 = 69.6$ mN/m at 40 °C). This method can also be used to determine the cmc.

Figure 10 shows the time-dependent surface pressure increase during the adsorption process of $(PGMA_{14})_2-PPO_{34}$ (Figure 10a) and $(PGMA_{221})_2-PPO_{34}$ (Figure 10b) at the air−water interface after being injected at the bottom of the circular trough with stirring at 40 °C.

When only a small volume of the polymer solution was injected, there was an induction period where no significant increase in surface pressure occurs. For higher concentrations such induction period does not exist and a steep increase of π is observed. In all cases a constant π value is reached at the plateau region of the isotherms. The time for reaching this value depends on the concentration and on the length of the PGMA blocks. For $(PGMA_{14})_2-PPO_{34}$ it varies between 6 min (for a total concentration in the trough of 63 μM) and around 4 h (for a total concentration of 130 nM). As could be expected the absorption at the air−water interface for the bulkier $(PGMA_{221})_2-PPO_{34}$ takes longer, ranging from 40 min (for a total concentration of 50 μM) and around 5 h (for a total concentration of 510 nM). It can be seen from Figure 10 that above a certain concentration the plateau values are constant due to the fact that the cmc is reached. Therefore, the cmc can also be determined from this type of measurement. The values obtained

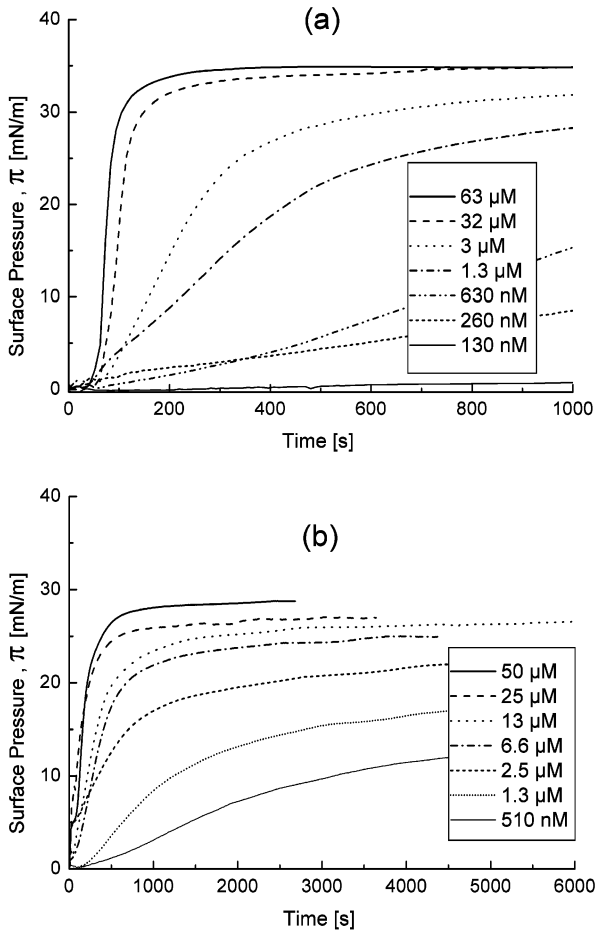

Figure 10. Time-dependent surface pressure increase during the adsorption process of (a) $(PGMA_{14})_2-PPO_{34}$ and (b) $(PGMA_{221})_2-PPO_{34}$ at the air−water interface after being injected at the bottom of a circular trough with stirring at 40 °C. The corresponding total concentration of the triblock copolymer in the trough for each experiment is given in the legend.

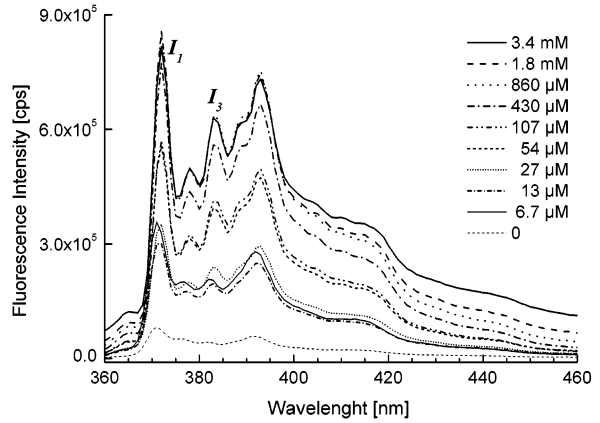

Figure 11. Emission spectra of pyrene (5.4×10^{-7} M) in aqueous solutions in the presence of different concentrations of $(PGMA_{15})_2-PPO_{34}$. Noteworthy is the change in the intensity ratio of the first (I_1) and third (I_3) pyrene vibrational bands. $\lambda_{ex} = 333$ nm.

from these experiments are in agreement with those obtained by the first method.

Fluorescence Studies. The pyrene solubilization technique has been used previously for the determination of the cmc in block copolymer solutions.[39,44] The pyrene fluorescence is sensitive to changes in the microenvironment which permits monitoring its incorporation into micelles at concentrations exceeding cmc. Figure 11 shows typical emission spectra of

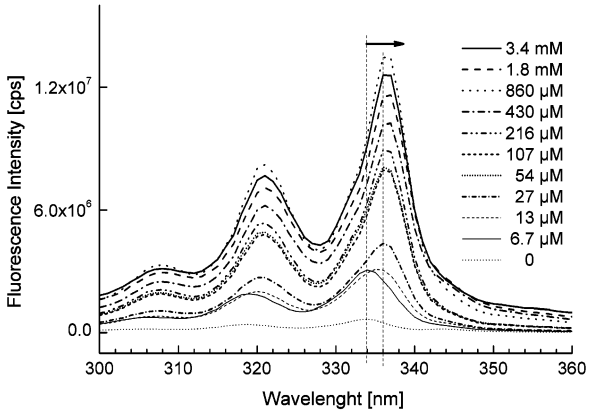

Figure 12. Excitation spectra of pyrene (5.4×10^{-7} M) in aqueous solutions, monitored at $\lambda_{em} = 390$ nm, in the presence of different concentrations of $(PGMA_{15})_2-PPO_{34}$, showing the shift in the (0,0) band as pyrene partitions between aqueous and micellar environments.

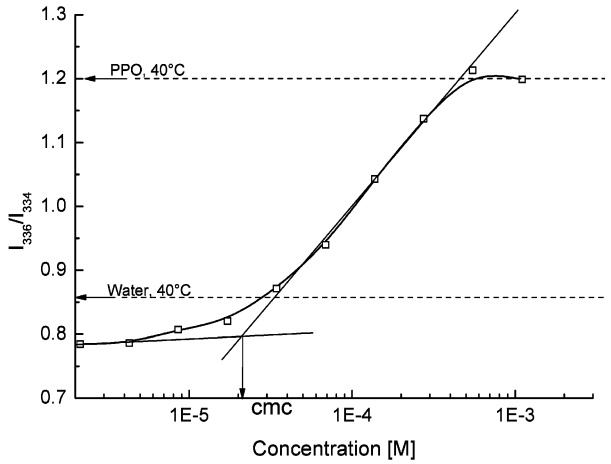

Figure 13. Intensity ratio I_{336}/I_{334} from pyrene excitation spectra as a function of $(PGMA_{221})_2-PPO_{34}$ concentration at 40 °C.

pyrene (5.4×10^{-7} M) in the presence of different concentrations of $(PGMA_{15})_2-PPO_{34}$. Figure 12 shows the corresponding pyrene excitation spectra. Both kinds of spectra, emission and excitation, are characteristic of pyrene monomer fluorescence in specific microenvironments. With increasing PGMA−PPO−PGMA concentration in the aqueous solution of pyrene, the intensity ratio between the first and the third vibrational band (I_1/I_3) in the emission spectra decreases from 1.9, typical of pyrene in water, down to around 1.3 indicating the location of pyrene in a hydrophobic environment. On the other hand, a shift of the (0,0) band in the excitation spectra from 334 to 336 nm is observed. This shift accompanies the transfer of pyrene molecules from a water environment to the hydrophobic micellar cores and thus provides information on the location of the pyrene probe in the system. Thus, the intensity ratio I_{336}/I_{334} of the (0,0) band of pyrene serves as a measure of the polarity of the environment and therefore is sensitive to the onset of micellization.[27] This ratio varied from 0.86 for water to 0.98 for PGMA and 1.20 for a PPO aqueous solution, all measured at 40 °C. A plot of the intensity ratio I_{336}/I_{334} from the excitation spectra as a function of $(PGMA_{221})_2-PPO_{34}$ concentration is shown in Figure 13. The cmc values were taken as the intersection of straight line segments, drawn through the points at the lowest polymer concentrations, which lie on a nearly horizontal line, with that going through the points on the rapidly rising part of the plot. (see Figure 13). The cmc values found are given in Table 2.

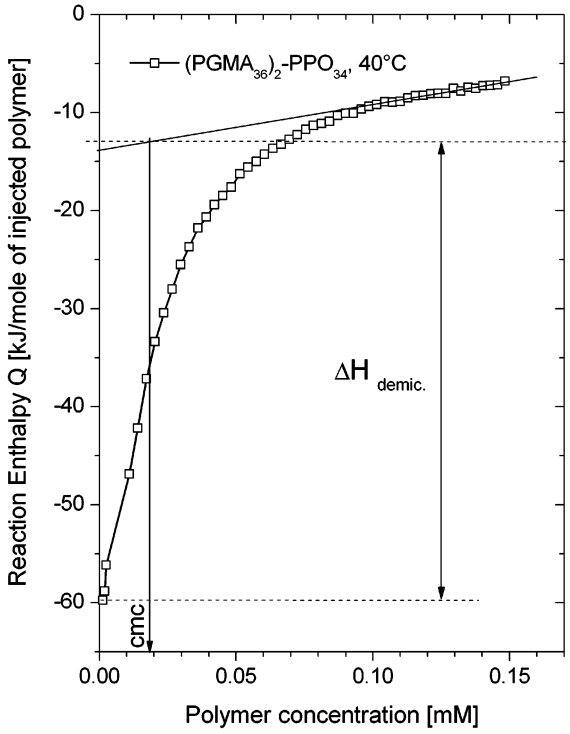

Figure 14. Determination of the enthalpy of demicellization, $\Delta H_{demic.}$ and the cmc from the experimental enthalpograms obtained by titration of a 1 mM $(PGMA_{36})_2-PPO_{34}$ solution into water at 40 °C (step size 5 μL).

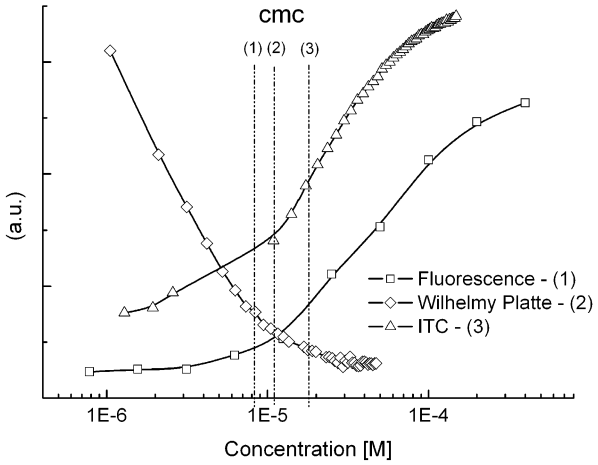

Figure 15. Determination of cmc values by different techniques for $(PGMA_{36})_2-PPO_{34}$ in water at 40 °C. Measured quantities: (1) fluorescence, intensity ratio I_{336}/I_{334} from pyrene excitation spectra; (2) Wilhelmy plate, surface tension (γ); (3) ITC, ΔH demicellization.

Isothermal Titration Calorimetry (ITC) Studies. Analysis of the ITC Enthalpograms. ITC is a widely used method to determine cmc values of surfactants. Its advantage is the parallel determination of the micellization enthalpy and the cmc, from which the free energy of micellization can be determined.[45−47]

Normally asymmetric sigmoidal titration curves are obtained and the enthalpy of micellization is obtained from the step height. As the enthalpograms obtained here did not present clear sigmoidal features, the enthalpy of demicellization, $\Delta H_{demic.}$, is more difficult to determine. We took the difference between the linearly extrapolated upper curve into the cmc region and the first values of the titration enthalpy as the demicellization enthalpy $\Delta H_{demic.}$ (see Figure 14). The cmc value was estimated by taking the concentration value at the half-height of the enthalpogram. All demicellization enthalpies were negative. For

the demicellization of low molecular weight surfactants a strong temperature dependence of the demicellization enthalpy is usually observed with a specific temperature where ΔH_{demic} is zero.[45] This specific temperature is higher for surfactants with large polar groups and the demicellization enthalpy at constant temperature becomes more negative for surfactants with larger polar groups. A similar effect seems to apply for the block copolymers, i.e., $(PGMA_{36})_2-PPO_{34}$ has a more negative demicellization enthalpy than the block copolymers with the shorter PGMA segments.

Determination of the Thermodynamic Parameters. The value of the critical micellization concentration (cmc) of a nonionic surfactant in aqueous solution has been widely used to determine the free energy of micellization of the surfactant, $\Delta G_{mic.}$, that is, the standard Gibbs free energy of transfer of a polymer chain from the water phase into a micelle, using the relationships:[48]

$$\Delta G^\circ_{mic.} = RT\,(\ln cmc) \tag{2}$$

The change in entropy $\Delta S_{mic.}$, can easily be obtained using the Gibbs−Helmholtz equation:[49]

$$\Delta S^\circ_{mic.} = (\Delta H^\circ_{mic.} - \Delta G^\circ_{mic.})/T \tag{3}$$

The term $\Delta G^\circ_{mic.}$ was calculated from the cmc values, expressed in polymer mole fraction, and eq 2, and ΔS°_{mic} was derived from eq 3. The measured cmc values and the corresponding thermodynamic parameters are given in Table 2.

When comparing the cmc values obtained from the different techniques used (see Figure 15), a satisfactory agreement is found, with all values lying within an order of magnitude of the cmc scale. The differences can be partially ascribed to the inherent different sensitivity of each method, the fluorescent probe method being more sensitive to the association onset.

Conclusions

Novel water-soluble PGMA−PPO−PGMA triblock copolymers were successfully synthesized via the ATRP technique. Unimodal molar mass distributions and relatively low polydispersities were obtained for different lengths of the PGMA block. Their association behavior in aqueous solutions was studied. Triblock copolymers having PGMA blocks with a degree of polymerization around half of that of the PPO block formed micelles with a well-defined and practically constant size of $R_h \sim 10-15$ nm in the temperature range of 15−40 °C and exhibited a critical micellization temperature at about 8 °C, above which micelles could be formed. Copolymers having PGMA blocks of length comparable to that of the PPO block exhibited a critical micellization temperature at about 19 °C. Also aggregates with sizes in the range of $R_h \sim 175-215$ nm were formed at temperatures below cmt. Triblock copolymers having much longer PGMA blocks where present mostly as unimers. Critical micellization concentrations (cmc) were determined using surface tension measurements, fluorescent probe technique with pyrene as probe molecule and isothermal titration calorimetry (ITC). A relatively good agreement was found between the cmc values obtained from the different methods.

Acknowledgment. We thank the "Deutsche Forschungsgemeinschaft" (DFG) for financial support through Programs GK-894 and SFB-418.

Supporting Information Available: Text describing the procedure for and figures showing AF4 fractograms, mass weighted distributions of R_h, and Γ vs q^2 and a table of molar mass data. This material is available free of charge via the Internet at http://pubs.acs.org.

References and Notes

(1) Alexandridis, P.; Lindman, B. In *Amphiphilic block copolymers*, 1st ed.; Alexandridis, P., Lindman, B., Eds.; Elsiever Science: Amsterdam, 2000; p 10.
(2) Kabanov, A.; Alakhov, V. In *Amphiphilic block copolymers*, 1st ed.; Alexandridis, P., Lindman, B., Eds.; Elsiever Science: Amsterdam, 2000; p 349.
(3) Erukova, V.; Krylova, O.; Antonenko, Y.; Melik-Nubarov, N. *Biochim. Biophys. Acta* **2000**, *1468*, 73−86.
(4) Kabanov, A.; Batrakova, E.; Alakhov, V. *Adv. Drug Delivery Rev.* **2002**, *54*, 759−779.
(5) Sunhee, C.; Jhon, M. S.; Andrade, J. D. *J. Colloid Interface Sci.* **1977**, *61*, 1−8.
(6) Gates, G.; Harmon, J. P.; Ors, J.; Benz, P. *Polymer* **2003**, *44*, 207−214.
(7) Gates, G.; Harmon, J. P.; Ors, J.; Benz, P. *Polymer* **2003**, *44*, 215−222.
(8) Leung, B. K.; Robinson, G. B. *J. Appl. Polym. Sci.* **1993**, *47*, 1207−1214.
(9) Beers, K. L.; Boo, S.; Gaynor, S. G.; Matyjaszewski, K. *Macromolecules* **1999**, *32*, 5772−5776.
(10) Spanswick, J.; Matyjaszewski, K. *Mater. Today* **2005**, *12*, 901−915.
(11) Patten, T. E.; Matyjaszewski, K. *Adv. Mater.* **1998**, *8*, 26−33.
(12) Coessens, V.; Pintauer, T.; Matyjaszewski, K. *Prog. Polym. Sci.* **2001**, *26*, 337−377.
(13) Beinert, G.; Hild, G.; Rempp, P. *Makromol. Chem.* **1974**, *175*, 2069−2077.
(14) Mori, H.; Hirao, A.; Nakahama, S. *Macromolecules* **1994**, *27*, 35−39.
(15) Mori, H.; Hirao, A.; Nakahama, S.; Senshu, K. *Macromolecules* **1994**, *27*, 4093−4100.
(16) Liu, F.; Liu, G. *Macromolecules* **2001**, *34*, 1302−1307.
(17) Pilon, N. L.; Armes, S. P.; Findlay, P.; Rannard, S. P. *Langmuir* **2005**, *21*, 3808−3813.
(18) Zhu, Z.; Armes, S. P.; Liu, S. *Macromolecules* **2005**, *38*, 9803−9812.
(19) Weaver, J. V.; Bannister, I.; Robinson, K. L.; Bories-Azeau, X.; Armes, S. P.; Smallridge, M.; McKenna, P. *Macromolecules* **2004**, *37*, 2395−2403.
(20) Liu, S.; Weaver, J. V.; Save, M.; Armes, S. P. *Langmuir* **2002**, *18*, 8350−8357.
(21) Zhang, Z.; Liu, G.; Bell, S. *Macromolecules* **2000**, *33*, 7877−7883.
(22) Oguchi, K.; Sanui, K.; Ogata, N.; Takahashi, Y.; Nakada, T. *Polym. Eng. Sci.* **1990**, *30*, 449−452.
(23) Wang, X. S.; Jackson, R. A.; Armes, S. P. *Macromolecules* **2000**, *33*, 255−257.
(24) Jankova, K.; Chen, X. Y.; Kops, J.; Batsberg, W. *Macromolecules* **1998**, *31*, 538−541.
(25) Liu, S.; Armes, S. P. *J. Am. Chem. Soc.* **2001**, *123*, 9910−9911.
(26) Hussain, H.; Busse, K.; Kressler, J. *Macromol. Chem. Phys.* **2001**, *202*, 3403−3409.
(27) Astafieva, I; Zhong, X. F.; Eisenberg, A. *Macromolecules* **1993**, *26*, 7339−7352.
(28) Save, M.; Weaver, J. V.; Armes, S. P.; McKenna, P. *Macromolecules* **2002**, *35*, 1152−1159.
(29) Wang, J.; Grimaud, T.; Matyjaszewski, K. *Macromolecules* **1997**, *30*, 6507−6512.
(30) Matyjaszewski, K.; Wang, J.; Grimaud, T; Shipp, D. *Macromolecules* **1998**, *31*, 1527−1534.
(31) Matyjaszewski, K.; Shipp, D.; Wang, J. A.; Grimaud, T.; Patten, T. E. *Macromolecules* **1998**, *31*, 6836−6840.
(32) Matyjaszewski, K.; Wang, J.; Grimaud, T; Shipp, D. *Macromolecules* **1998**, *31*, 1527−1534.
(33) Craven, J. R.; Tyrer, H.; Booth, C.; Jackson, D. *J. Chromatogr.* **1987**, *387*, 233−240.
(34) Feng, X.; Pan, C.; Wang, J. *Macromol. Chem. Phys.* **2001**, *202*, 3403−3409.
(35) Hadjichristidis, N.; Pispas, S.; Floudas, G. In *Block copolymers*; 1st ed.; Wiley-Interscience: New York, 2003; p 214.
(36) Garnaik, B.; Thombre, M. S. *J. Appl. Polym. Sci.* **1999**, *72*, 123−133.
(37) Okaya, T. In *Polyvinylalcohol developments*, 1st ed.; Finch, C. A., Ed.; John Wiley & Sons: Chichester, U.K., 1992; p 4.
(38) Gerle, M.; Fischer, K.; Roos, S.; Müller, A.; Schmidt, M. et. al. *Macromolecules* **1999**, *32*, 2629−2637.

(39) Kavanov, A.; Nazarova, I.; Astafieva, I.; et. al. *Macromolecules* **1995**, *28*, 2303−2314.
(40) Zhou, Z.; Chu, B. *Macromolecules* **1988**, *21*, 2548−2554.
(41) Glatter, O.; Scherf, G.; Schillén, K.; Brown, W. *Macromolecules* **1994**, *27*, 6046−6054.
(42) Booth, C.; Attwood, D. *Macromol. Rapid Commun.* **2000**, *21*, 501−527.
(43) Hussain, H.; Kerth, A.; Blume, A.; Kressler, J. *J. Phys. Chem. B* **2001**, *105*, 3105−3108.
(44) Wilhelm, M.; Zhao, C. L.; Wang, Y.; Xu, R.; Winnik, M. A. *Macromolecules* **1991**, *24*, 1033−1040.
(45) Paula, S.; Süs, W.; Tuchtenhagen, J.; Blume, A. *J. Phys. Chem.*. **1995**, *99*, 11742−11751.
(46) Garidel, P.; Hildebrand, A.; Neubert, R.; Blume, A. *Langmuir* **2000**, *16*, 5267−5275.
(47) Majhi, P. R.; Blume, A. *Langmuir* **2001**, *17*, 3844−3851.
(48) Zana, R.; *Langmuir* **1996**, *12*, 1208−1211.
(49) Bai, G.; Wang, J.; Yan, H.; Li, Z.; Thomas, R. K. *J. Phys. Chem. B* **2001**, *105*, 3105−3108.

MA060794N